JOURNAL OF MATERIALS SCIENCE 28 (1993) 2067–2074

Analysis of the formation and removal of gas bubbles in rotationally moulded thermoplastics

L. XU, R. J. CRAWFORD
Department of Mechanical and Manufacturing Engineering, The Queen's University of Belfast, Belfast BT9 5AH, UK

The presence of internal bubbles is a characteristic feature of thermoplastic products manufactured by rotational moulding. The bubbles in the mouldings are generally undesirable since they reduce strength and stiffness and impair the appearance of the product if they occur at the surface. The bubbles form as a result of powder particles coalescing during the heating stage of the process and they subsequently decrease in size as a function of time and temperature. This paper presents a semi-empirical model to predict the bubble size which is likely to occur under any specified processing conditions.

Nomenclature

r_0 Initial radius of bubble at time $t = 0$ (mm)
r Radius of bubble at any time t (mm)
ξ Distance from the centre of the bubble at time t (mm)
x Neck radius of two spheres (mm)
γ Surface tension ($N\,cm^{-1}$)
P pressure inside the bubble ($N\,cm^{-2}$)
η Viscosity at time t ($N\,s\,m^{-2}$)
η_0 Initial viscosity ($N\,s\,m^{-2}$)
t Time
K Experimental constant
τ Apparent relaxation constant
Q Quantity of oxygen in the bubble (cm^3)
ϕ Diameter of the bubble (mm)
ϕ_0 Initial diameter of the bubble (mm)
ρ_p Density of the polymer
ρ_b Density of the bubble
u Terminal velocity of the bubble
g Acceleration due to gravity
J Solute flux
c Concentration of dissolved oxygen in the glass at a distance ξ from the centre of the bubble at time t
c_0 Constant concentration maintained at the surface of bubble in equilibrium with oxygen gas at 1 atm inside the bubble
α Diffusion coefficient
c_s Concentration of solute in the sphere
c_i Concentration of solute in the solution at the sphere–solution interface
c_∞ Solute concentration at a large distance from the sphere

1. Introduction

Rotational moulding is a processing technique which competes with injection moulding, blow moulding and vacuum forming in the production of hollow thermoplastic articles. During the rotomoulding process, a relatively inexpensive mould is charged with a pre-weighed amount of plastic powder (or liquid) and then heated whilst being rotated about two perpendicular axes in an oven [1]. The powder melts and adheres to the wall of the rotating mould, which is subsequently cooled whilst the biaxial rotation continues. Finally, the mould is opened, the part removed, and the mould recharged for the next cycle. With the increasing demands on rotational moulding, there is a need for much better understanding of the basic technology of the process. Although rotomoulding appears simple, the plastic powder undergoes complex flow and melt processes. There are several major areas which are not well understood about the rotational moulding process. One of these is the formation of bubbles in the wall section of the moulding and their subsequent removal as the melt/mould continues to rotate in the oven. The presence of bubbles in the moulding is a vital factor in the rotomoulding process because it has a major effect on the final properties of the product. In relatively thin products, the bubbles can be completely removed but this can result in polymer degradation due to the extended time or elevated temperatures which are required. Generally the moulder will set the cycle time such that some bubbles are retained and thus degradation is avoided. It has been shown conclusively that degraded material suffers a drastic drop in impact strength [2]. It is of considerable importance therefore to be able to predict the size of bubbles likely to occur for any selected process conditions, in order that cycle times and product properties can be optimized.

The presence of bubbles rotomoulded parts has been examined over many years [1–6]. A detailed analysis of bubble formation and removal during centrifugal casting of metals has been described by Spencer [7]. He concluded that when filling any

0022–2461

cavity, the trapping of gas pockets is unavoidable. He asserted that the bubbles are removed essentially by increasing the buoyancy forces. Thus, the larger a bubble, the greater its buoyancy and hence the faster it proceeds through the melt to the free surface.

It is to be expected that the qualities of products will be at their best when all bubbles have been removed from the moulded parts [8, 9]. However, it has been found that there is a relatively sharp transition from ductile to brittle behaviour close to the point when the bubbles disappear. Most moulders tend to err on the side of caution and prefer to retain some bubbles in the final product. Although polyethylene is the major rotomoulding material, the problem of moulded-in bubbles is not restricted to this material. The problem has been found to be particularly bad in the polycarbonate, nylon and ABS materials although predrying of the feedstock reduces the effects [10, 11].

There are many factors which have been identified as contributing to the presence of gas bubbles [3, 6, 12–23]. These include particle shape and size, particle size distribution, melt flow index, volatiles, moisture, small pores in the mould surface, material degradation, mould design, and the heating and cooling cycles during the rotomoulding process.

Many authors have referred to the presence of bubbles in rotomoulded parts. However, only a few have made an attempt to understand the problem [24–26]. Rao and Throne [24] suggested in early work that the formation of a homogenous melt from powder particles involves two distinct stages. The first involves the formation of interfaces and bridges between adjacent particles with little change in density. Secondly, there is a stage of densification in which the interparticle cavities are filled with molten polymer which is drawn into the region by capillary action. Rao and Throne used this model to explain the "pockmarks" on the surface of mouldings. It was suggested that these are caused by the voids in the powder interior being pushed ahead of the melt front to the free surface. This work involved an analysis of buoyancy, capillary and hydrodynamic forces in relation to the surface tension forces which are opposing them.

Ten years later, Progelhof *et al.* [25] developed this theory further. Their more modern theory suggested that as the powder is heated, the particles become sticky and adhere to each other, and upon further heating the particles fuse together or densify to form a unitized structure. As the heating process continues, the solid–melt interface moves upwards, the top of the free surface of the powder drops and eventually the powder completely melts. The voids appear to be a result of a bound inclusion of the space between individual particles, and the most striking point was the slow movement of voids to the free surface. There appeared to be some coalescence of the voids but with time the voids diminished in size.

Kelly [26] also considered powder densification but in this case the approach was different. Kelly suggested that air bubbles are trapped in the polymer during melting and decrease in diameter as the polymer melt temperature increases. The high viscosity of the melt prevents the movement of the bubbles. At a high enough melt temperature, the air in the bubbles begins to dissolve into the polymer. Oxygen has about twice the solubility of nitrogen in polyethylene. At high temperatures, the oxygen is further depleted by direct oxidation reactions with polyethylene. The depletion of oxygen reduces the bubble diameter. The laws of surface tension dictate that the pressure inside the bubble has to increase as the diameter decreases. The increase in pressure forces the nitrogen to dissolve in the polymer, thus the bubble diameter is further reduced and this chain of events repeats until the bubble disappears. As the cycle time increases, the bubble diminishes in size and the number of bubbles decreases. At very long cycle times, the moulded part will have no bubbles. However, as indicated earlier, impact strength is found to be low because the polymer has oxidized – presumably as a legacy of the oxygen in the bubbles [2].

Kelly [26] also refers to a critical bubble size above which the gases will not dissolve regardless of temperature or time because the surface tension forces cannot generate a high enough bubble pressure to help dissolve the gases inside the bubble. Extensive experimental work by Crawford and Scott [6] has confirmed the Kelly model. Using a video camera to record the formation and removal of the bubbles it was possible to derive an equation to predict the bubble size under isothermal conditions. This work has now been further refined to recognise that the formation/removal of the bubbles is in fact a time–temperature phenomenon and so a much more general equation has been proposed.

2. Theory

Once a gas pocket has formed inside the polymer melt, three main factors affect the rate of diameter decrease:

(i) diffusion of the gas at the surface of the bubble,
(ii) diffusion of this dissolved gas away from the bubble into the polymer melt and
(iii) buoyancy forces on the bubble.

It seems likely that at high temperature effect (i) is rapid, and what predominantly determines the overall rate of solution of the bubble is the diffusion of dissolved oxygen away from the bubble. These three main factors will be described mathematically in the next section.

2.1. Sintering

To understand the bubble formation and removal mechanism, it is necessary to understand the process of polymer sintering and densification. A mathematical treatment of the sintering process is described below.

Solid particles, when in contact with each other at elevated temperatures, tend to decrease their total surface area by coalescence. This process, called sintering, is usually accompanied by a decrease of the total volume of the powder mass. A decrease in surface area brings about a decrease in (surface) free energy.

Thus the surface tension is the predominant force for the coalescence process.

Frenkel [27] was the first person to consider the concept of viscous sintering, and derived an expression for the rate of coalescence of adjacent spheres under the action of surface tension. From the model given in Fig. 1, he developed a theory which predicts the variation of the sintering process with time for two identical spheres. The Frenkel expression takes the form

$$\frac{x^2}{r} = \frac{3}{2}\left(\frac{\gamma}{\eta}\right)t \tag{1}$$

where x is the neck radius as represented schematically in Fig. 1, r is the radius of the spheres, γ is the surface tension, η is the viscosity and t is the time. This relationship has been confirmed by Kuczynski and Zaplatynskyj [28] for the sintering of glass. For the second stage of the sintering process, normally described as densification, these authors were able to derive an equation of the form

$$r_0 - r = \frac{\gamma t}{2\eta} \tag{2}$$

where r_0 is the initial radius of the pore and r is the reduced radius at time t. This expression was applied successfully to glass and ceramic materials, but for polymeric materials Kuczynski *et al.* [29] and others [30–34], working with polymethylmethacrylate, found that the experimental data conformed to the general expression

$$\left(\frac{x^2}{r^{1.02}}\right)^n = K(T)t \tag{3}$$

where K is an experimental constant, T the temperature, t the sintering time, r the radius of the PMMA sphere and x the radius of interface. The exponent n decreases from 5 to approximately 0.5 as the sintering temperature increases from 127 to 207 °C.

In 1962, Lontz [35] studied the sintering of polytetrafluoroethylene and suggested that for viscoelastic sintering, the time-dependent interfacial (x/r) coalescence should be more properly described as

$$\frac{x^2}{r} = \frac{3}{2}\left(\frac{\gamma t}{\eta_0(1 - e^{-t/\tau})}\right) \tag{4}$$

where η_0 represents the initial viscosity and τ is an apparent relaxation constant to be assigned from experimental determinations to account for both inherent and stress-induced retardation.

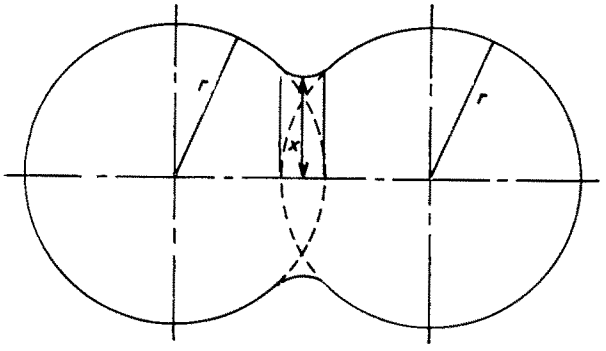

Figure 1 Model for sintering concept. Two spheres of radius r form a contact area of radius x.

As the sintering proceeds and coalescence and densification occur, the overall heat conduction problem does not remain unaffected. Clearly, the effective thermophysical properties change, influencing the overall temperature distribution, and hence the local sintering problem as well.

2.2. Mathematical treatment of the diffusion of gas from a spherical bubble into the surrounding polymer

The rate at which a gas bubble in a polymer at constant temperature shrinks or expands may be assumed to depend on the rate at which the gas dissolves in the polymer melt at the surface of the bubble or is evolved from the polymer into the bubble.

As the temperature of the polymer melt increases, the oxygen in the air bubble begins to dissolve in the polymer. As stated earlier, oxygen has about twice the solubility of nitrogen in polyethylene. At the higher temperature, the oxygen is further depleted by direct oxidation reactions with polyethylene. The depletion of oxygen reduces the bubble diameter and increased the pressure in the bubble. The laws of surface tension dictate that the pressure inside the bubble has to increase as the diameter decreases. Hence

$$P = K\left(\frac{2\gamma}{r}\right) \tag{5}$$

where P is the pressure inside the bubble ($N\,cm^{-2}$), γ is the surface tension ($N\,cm^{-1}$) r is the radius of the bubble (mm) and K is a constant. It can be seen that the increase in pressure in the bubble due to surface tension is inversely proportional to the diameter of the bubble.

The radius r of the bubble at any time t with a bubble of initial radius r_0 is determined by the diffusion constant α of dissolved oxygen in the polymer and by the solubility c_0 of oxygen at 1 atm in the polymer, measured above the initial uniform concentration of dissolved oxygen. The differential equation for the diffusion of oxygen away from the bubble is given by Fick's law.

$$\frac{\partial c}{\partial t} = \alpha \nabla^2 c \tag{6}$$

where c is the concentration of the dissolved oxygen at a distance from the centre of the bubble at time t and α is the diffusion coefficient. It should be noted that Fick's diffusion law is for a single bubble in an infinite liquid. In reality there are many bubbles in close proximity and this may affect the diffusion mechanism.

If the problem is referred to a system of spherical coordinates with the origin at the centre of the bubble, it is evident that the concentration of dissolved oxygen does not depend on the angular coordinates but only on the distance ξ from the centre of the bubble. Thus,

the diffusion equation reduces to the form

$$\frac{\partial c}{\partial t} = \alpha \frac{\partial^2 (c\xi)}{\partial \xi^2} \tag{7}$$

where ξ is the distance from the centre of the bubble.

This equation is to be solved subject to the boundary condition that c is equal to c_0 on the surface of the bubble at all times. Here the complication arises that the radius of the bubble, r, on which this boundary condition $c = c_0$ holds, itself decreases with time in a way which depends on the solution of the diffusion problem. This is a type of problem known as a Stefan problem.

An approximation has been made by Greene and Gaffney [36] by imagining that oxygen is supplied to a bubble in some unspecified way for a time t at such a rate as to maintain the size of the bubble. For this diffusion problem where r, the radius of the bubble, is a constant, the exact solution may be obtained from standard tests. It is

$$c = \frac{c_0 r}{\xi}\left[1 - \exp\left(\frac{\xi - r}{2(\alpha t^{1/2})}\right)\right] \tag{8}$$

where c is the concentration of dissolved oxygen in the glass at a distance ξ from the centre of the bubble at time t, c_0 is the constant concentration maintained at the surface of bubble in equilibrium with oxygen gas at 1 atm inside the bubble, r is the radius of the bubble and α is the diffusion coefficient.

At any time t, the rate at which oxygen leaves the bubble is determined by the concentration gradient at the surface of the bubble:

$$\frac{dQ}{dt} = \alpha A \left(\frac{\partial c}{\partial \xi}\right)_{\xi = r} \tag{9}$$

Here Q is the quantity of oxygen in the bubble measured in cm^3 at the temperature of the experiment. c is the concentration of dissolved oxygen, which is measured in cm^3 of gas at the temperature in question per cm^3 of polymer. A is the surface area of the bubble which is equal to $4\pi r^2$.

The concentration gradient at the surface is obtained by differentiating Equation 9 with respect to ξ:

$$\left(\frac{\partial c}{\partial \xi}\right)_{\xi = r} = -c_0\left(\frac{1}{r} + \frac{1}{(\pi\alpha t)^{1/2}}\right) \tag{10}$$

Since the quantity of oxygen contained in the bubble, Q, is equal to $4\pi r^3/3$, Equation 5 will give the rate at which the bubble would start shrinking if the imaginary internal supply of oxygen, which previously maintained its radius constant at r, were suddenly cut off at time t. If it is now assumed that the concentration gradient of a bubble which has actually shrunk to the radius r at time t is the same as that of a bubble which has been maintained at radius r by an internal supply of oxygen for the same time t, then a differential equation connecting the radius of the shrinking bubble r with the time may be obtained. This approximate solution of the Stefan problem is

$$\frac{d}{dt}\left(\frac{4}{3}\pi r^3\right) = \alpha(4\pi r^2)\left[-c_0\left(\frac{1}{r} + \frac{1}{(\pi\alpha t)^{1/2}}\right)\right] \tag{11}$$

or

$$\frac{dr}{dt} = -\alpha C_0\left(\frac{1}{r} + \frac{1}{(\pi\alpha t)^{1/2}}\right) \tag{12}$$

Equation 12 may be solved by standard methods and the constant of integration evaluated by setting r equal to the initial radius of the bubble r_0 at $t = 0$. If c_0, the solubility of oxygen in the polymer, measured in volume of gas per volume of polymer is less than 2π, the resulting equation for r as a function of t is

$$\ln\left(\xi^2 + \frac{2c_0 r(\alpha t)^{1/2}}{\pi^{1/2}} + 2c_0\alpha t\right) + 2\left(\frac{c_0}{2\pi - c_0}\right)^{1/2} \times \left[\cot^{-1}\left(\frac{c_0}{2\pi - c_0}\right)^{1/2}\right]\left(\frac{(\pi r)^{1/2}}{c_0(\alpha t)^{1/2}} + 1\right) = 2\ln r_0 \tag{13}$$

when t is small so that $r \gg (\pi\alpha t)^{1/2}$ Equation 12 has an approximate solution

$$r = r_0 - \frac{2c_0}{\pi^{1/2}}(\alpha t)^{1/2} \tag{14}$$

This same limiting form for small values of t may be obtained by expanding the ln and $\cot^{-1}$ functions in Equation 13. When r becomes small, another limiting solution of Equation 12 may be obtained which is useful in plotting Equation 13. It has the form

$$r^2 = k - 2\pi\alpha t \tag{15}$$

Equation 12 evidently leads to a decrease in bubble size proportional to the square root of time in the initial stages of the shrinking of the bubble, followed by a more and more rapid shrinking in the later stages.

Unfortunately, this approximate solution may be shown to predict shrinking which is too rapid in the later stages of dissolution of a bubble. This may be seen by considering another approximate solution of the problem. In this case it is supposed that the original bubble of radius r_0 loses gas by diffusion for time t. If it is then allowed to shrink suddenly to radius r, conservation of polymer volume will cause the separation $\Delta\xi$ between concentric spherical surfaces of radius ξ and $\xi + \Delta\xi$ on which the concentration of dissolved oxygen are c and $c + \Delta c$ to increase in proportion to the square of the reciprocal of ξ. Hence the concentration gradient at the surface of the bubble will decrease in proportion to the square of its radius. Then

$$\left(\frac{\partial c}{\partial \xi}\right)_{\xi = r} = -c_0\left(\frac{1}{r_0} + \frac{1}{(\pi\alpha t)^{1/2}}\right)\frac{r^2}{r_0^2} \tag{16}$$

This yields a differential equation for r as a function of t

$$\frac{dr}{dt} = \frac{c_0\alpha}{r_0^2}\left(\frac{1}{r_0} + \frac{1}{(\pi\alpha t)^{1/2}}\right)r^2 \tag{17}$$

which has the solution

$$\frac{1}{r} - \frac{1}{r_0} = \frac{c_0}{r_0^2}\left[\frac{\alpha t}{r_0} + 2\left(\frac{\alpha t}{\pi}\right)^{1/2}\right] \tag{18}$$

These two approximate solutions illustrate the effects of two opposing influences on the rate of solution of oxygen from the shrinking bubble. Equation 13 takes

into account the increasing ratio of surface to volume as the bubble becomes smaller, which causes the shrinking to become more rapid. Equation 18 takes into account the decrease in concentration gradient at the surface of the bubble which also results from its contraction, but which causes the shrinking to become slower. The net effect of both influences may then be expected to cause the shrinking of the bubble to follow rather closely the course predicted by Equation 14 for a large part of its life.

Presumably, the solubility of oxygen in the polymer decreases as the temperature is increased. This would mean that the factor c_0 in Equations 13 and 14 decreases. If the process is diffusion-limited, this means that there is a sufficient increase in α, aided by the absolute temperature factor, to overcome the effect of c_0 and result in a net increase in the rate of shrinking of the bubbles.

From the foregoing, it is evident that more work is needed, extending over a greater temperature range and with more attention to the critical points in the history of the bubble (i.e. to the initial slow period and to the point when shrinking stops and the residual bubble remains). Some technique for recovering and analysing the residual bubble of insoluble gas also would be most desirable.

2.3. The buoyancy force of a bubble

The bubble, having formed, remains virtually stationary in the melt. A force analysis on the bubble shows that this is a reasonable statement:

$$\text{Buoyancy} = \text{weight of bubble} + \text{resisting force}$$

$$\frac{\pi\phi^3}{6}\rho_p g = \frac{\pi\phi^3}{6}\rho_b g + 3\pi\eta_0 u\phi \qquad (19)$$

where ϕ is the diameter of the bubble, ρ_p the density of the polymer, ρ_b the density of the bubble, η_0 the zero-shear viscosity of the polymer, u the terminal velocity of the bubble and g the acceleration due to gravity. Crawford and Scott [6] assumed a typical bubble diameter of 0.25×10^{-3} m and found that the viscosity of the molten polyethylene is so large that the buoyancy forces acting on the bubble are insignificant.

3. Experimental work

Using a hotplate system and video camera as described by Crawford and Scott [6], a series of tests were conducted to observe bubble formation and removal for a wide range of times and temperatures. The experimental apparatus consisted of a Tecam Dri-Block DB-4 hotplate coupled to a Eurotherm 812 microprocessor-based programmable controller as a steady heat source and a steel ring (95 mm dia., 50 mm high) with a mild steel baseplate to contain the powdered plastic. This container had a small section at the front removed to permit the insertion of a glass viewing window. The window permitted the powder to be observed over the whole container depth. K-type (NiCr–NiAl) thermocouples were used to monitor the temperatures at heights of 3, 6 and 15 mm from the baseplate in the powder/melt. A thermocouple was welded directly to the surface of the baseplate to record the true rates of heating experienced by the powder. A video camera system was set up to record the melting and homogenization of the plastic powder. The size of bubbles, general bubble content, rate of dissolution/disappearance, temperatures at base and at different heights can all be measured very conveniently using this equipment.

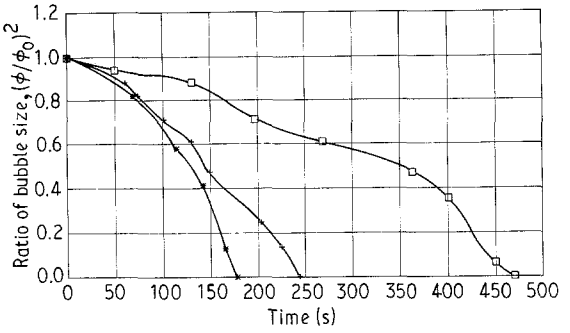

Figure 2 Experimental curves for bubble diameter ratio for hd-8760.27 resin: (■) 120 °C, (+) 160 °C, (∗) 190 °C.

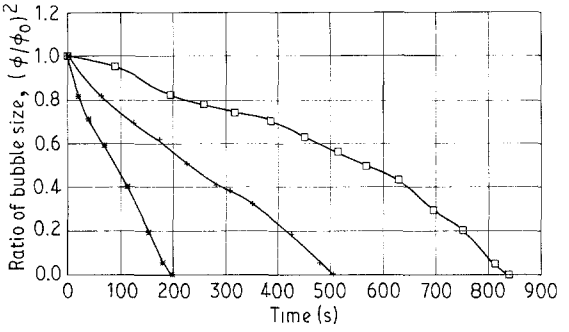

Figure 3 Experimental curves for bubble diameter ratio for LL-8461.27 resin: (■) 150 °C, (+) 170 °C, (∗) 200 °C.

The most suitable plastic for rotational moulding is polyethylene, due to its inherent thermal stability, excellent processing properties and low cost. Hence polyethylene was chosen as the material for the initial investigations of the bubble formation problem. Two grades of polyethylene were chosen: (a) high-density polyethylene. HD-8760.27 (lot 301-969) and (b) linear low-density polyethylene LL-8461.27 (lot 304-266), both supplied by Exxon Chemical International Marketing Inc. in Canada. The experimental data for bubble diameter as a function of time are shown in Figs 2 and 3.

4. Discussion and mathematical analysis

It can be seen from Figs 2 to 7 that the diffusion of the bubble into the polymer melt can be expressed as a function of temperature, time and initial bubble size. Initially, the bubble decreases in size at a relatively slow rate, but as the bubble diameter decreases, the area to volume ratio increases. This causes the pressure inside the bubble to increase and hence the diffusion process is assisted so that the rate of decrease of

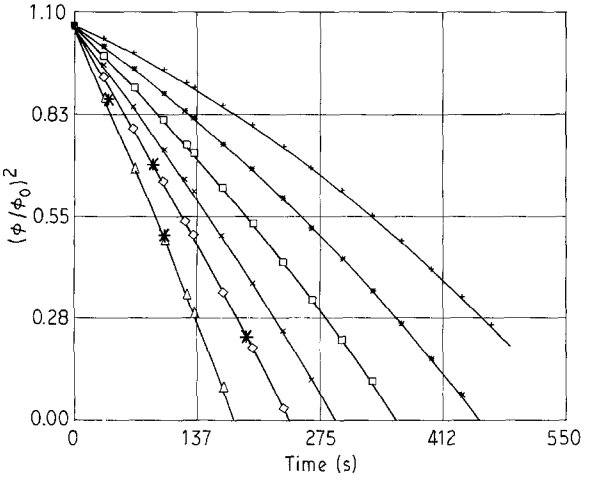

Figure 4 (——) Prediction curves with experimental data (symbols) for bubble diameter ratio as a function of time for HD-8760·27 resin: (+) 110 °C, (*) 125 °C, (□) 140 °C, (×) 150 °C, (◇), 175 °C.

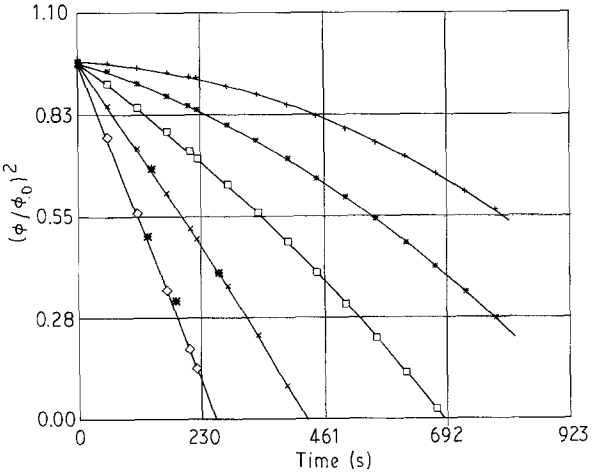

Figure 5 (——) Prediction curves with experimental data (symbols) for bubble diameter ratio as a function of time for U-8461.27 resin: (+) 120 °C, (*) 145 °C, (□) 160 °C, (×) 175 °C, (◇) 190 °C.

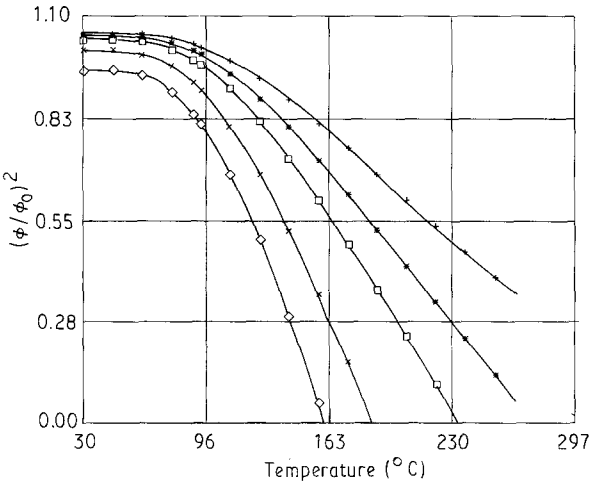

Figure 6 (——) Prediction curves with experimental data (symbols) for bubble diameter ratio as a function of temperature for HD-8760.27 resin: (+) 72 °C, (*) 100 °C, (□) 129 °C, (×) 196 °C, (◇) 269 °C.

diameter is accelerated. In order to quantify the effect of these variables, it is worth referring to the work by Doremus [37] and Green and Gaffney [36] who studied the diffusion of bubbles into glass. They found

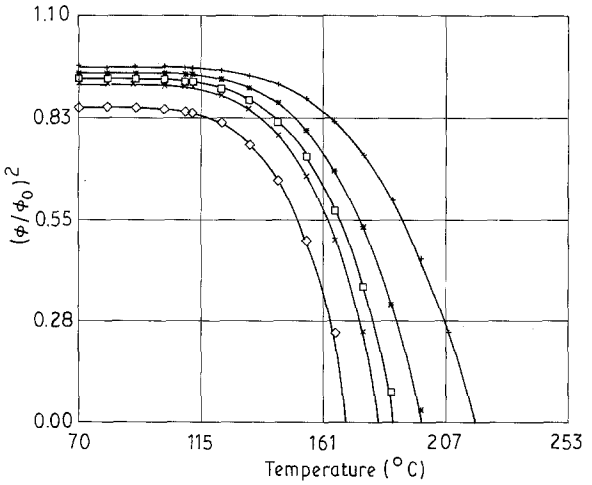

Figure 7 (——) Prediction curves with experimental data (symbols) for bubble diameter ratio as a function of temperature for U-8461.27 resin: (+) 110 °C, (*) 195 °C, (□) 260 °C, (×) 310 °C, (◇) 450 °C.

that the rate of shrinkage of the bubble was controlled by the diffusion of oxygen into the molten glass.

Greene and Gaffney [36] reported that there appears to be no rigorous solution of the diffusion equation for the case of a growing or shrinking sphere that has an appreciable initial radius. However, they found the bubble diameter was proportional to the square root of the time (see Equation 15).

Doremus [37] developed a modified form of the Green and Gaffney relationship. His primary interest was with the isothermal experimental state and he considered a sphere of radius r_0 at time $t = 0$ surrounded by a large amount of solution with a uniform solute concentration c_0. Under certain conditions the sphere will expand or contract with time. The radius of the sphere at time t is r. He made the following assumptions in order to derive the growth equations:

1. Diffusion of solute in the solution is the only process that affects the rate of growth or contraction of the sphere.
2. The concentration of solute in the sphere c_s is uniform and constant with time.
3. The concentration of solute in the solution at the sphere–solution interface, c_i, is uniform and constant with time.
4. The solution is large enough so that the solute concentration at a large distance from the sphere c_∞ equals $c_0 (c_\infty = c_0)$.
5. The diffusion coefficient α of the solute is constant with concentration and time.

Under these conditions the solute flux J per unit area and time at the surface of an isolated sphere of constant radius r_0 is given [38] by

$$J = \frac{(c_\infty - c_i)\alpha}{r_0}\left(1 + \frac{r_0}{(\pi\alpha t)^{1/2}}\right) \qquad (20)$$

with $c_0 = c_\infty$. For a growing sphere of zero initial radius in a dilute solution the rigorous result [39, 40] for J is

$$J = \frac{(c_\infty - c_i)\alpha}{r} \qquad (21)$$

A plausible equation for a growing or shrinking sphere of initial radius r_0 is therefore

$$J = \frac{(c_\infty - c_i)D}{r}\left(1 + \frac{r_0}{(\pi Dt)^{1/2}}\right) \quad (22)$$

in which r is now the total instantaneous radius of the sphere at any time t. This equation approaches Equation 21 when r_0 is small or t is large and approaches Equation 20 when r is nearly equal to r_0. For the case of a growing sphere, it can be seen that the present equation is preferable because the second term in parentheses should become negligible when $r_0 \ll (\pi Dt)^{1/2}$. Since $J = (c_s - c_i)dr/dt$, from Equation 22 the integrated growth equation is

$$r_0^2 - r^2 = 2D\beta t\left(1 + \frac{2r_0}{(\pi Dt)^{1/2}}\right) \quad (23)$$

where $\beta = (c_i - c_\infty)/(c_s - c_i)$; r_0 is the initial radius of the bubble, r the total instantaneous radius at any time t, α the diffusion coefficient and β the dimensionless gas concentration constant.

If $r_0 \ll (\pi\alpha t)^{1/2}$, as in the case for polyethylene [41], then the second term in parentheses becomes negligible and Equation 22 reduces to

$$\phi_0^2 - \phi^2 = K_1 t \quad (24)$$

where K_1 is a constant, $K_1 = 8\alpha\beta$ and ϕ_0 is the initial diameter. Rearranging gives

$$\left(\frac{\phi}{\phi_0}\right)^2 = 1 - K_2 t \quad (25)$$

where K_2 is a constant, $K_2 = 8\alpha\beta/\phi_0^2$.

Doremus [37] also found that the diffusion coefficient has a temperature dependency

$$\alpha = \alpha_0 \exp\left(-\frac{Q}{kT}\right) \quad (26)$$

where α_0 is the diffusion coefficient at time $t = 0$. So from Equation 25

$$\left(\frac{\phi}{\phi_0}\right)^2 = 1 - 8\alpha_0 \exp\frac{(-Q/KT)}{\phi_0^2} t = 1 - K_3 \times \exp\left(-\frac{K_4}{T}\right)t \quad (27)$$

where ϕ_0 is the initial bubble diameter, ϕ is the bubble diameter at time t and K_3, K_4 are constants.

It can be seen that the intercept is not in fact 1, although it is quite close to it. From the mechanism of bubble formation and removal and curve-fitting analysis of data obtained in the series of tests on polymers, it was found that for a gas bubble in a polymer melt it is probably more accurate to say that the following type of relationship applies:

$$\left(\frac{\phi}{\phi_0}\right)^2 = K_5 - K_2 t + K_6 t^2 \quad (28)$$

where K_6 is a constant, so the proposed model to determine the bubble size decrease with temperature and time is

$$\left(\frac{\phi}{\phi_0}\right)^2 = K_5 - K_3 \exp\left(-\frac{K_4}{T}\right)t + K_8 \exp\left(-\frac{K_7}{T^2}\right)t^2 \quad (29)$$

where K_5, K_7 and K_8 are constants. These constants are affected by the type of polymer, melt flow index, particle size, shape and particle size distribution, moisture, bubble initial diameter, temperature and heating rate.

In order to test the theory with regard to the nature of the above equation, a sophisticated data analysis package [42] was used to establish the "goodness of fit" and the appropriate constants when it is applied to the data in Figs 4 to 7. The computer program used for this data analysis incorporates a number of efficient optimization algorithms, as well as non-linear for sensitivity analysis and for plotting solutions. However, its effectiveness stems from the facility it provides for monitoring and controlling the solution process, for example by scaling or by changing the dimension of the problem, and also from the ease with which possible solutions can be analysed and verified. In the present case, the problem was so ill-conditioned that re-scaling was absolutely essential. Without it, the best fit obtainable had a sum of squares of residuals of about 10^6; by scaling all parameters to have equal magnitude in the optimization space this was ultimately reduced, in the case of LL-8461, to 0.054. Until it was reduced well below 1.0 no temperature effects were distinguishable, due to the low sensitivity of K_4 and K_7 compared with the other parameters.

Once the values of K_3, K_4, K_5, K_7 and K_8 had been determined, the computer program was used to predict bubble size for temperatures and times outside those in the experimental programme. For example, the prediction curves for 110, 125, 140, 155 and 175 °C for HD-8760.27 are shown in Fig. 4. The prediction curves for 120, 145, 160, 175 and 190 ° for LL-8461.27 are shown in Fig. 5. This model-fitting analysis can also give a prediction of bubble diameter ratio decrease rate versus temperature at any time. Fig. 6 shows the prediction curves for HD-8760.27 resin at 72, 100, 129, 196 and 269 s. Fig. 7 shows the prediction curves for LL-8461.27 resin at 110, 195, 260, 310 and 450 s.

Another four hotplate tests were done to identify the prediction curves. The tests were conducted at 140 and 175 °C for HD-8760.27 resin and at 160 and 190 °C for LL-8461.27 resin. The results are shown in Figs 4 to 7.

5. Conclusions

1. The rate of decrease of bubble diameter is dependent on the initial size of the bubble, the temperature of the melt, time, the type of polymer and the quantity of resin in the mould.

2. From the work reported here using the techniques described above, a semi-empirical relationship between bubble diameter ratio, temperature and time

has been developed. For HD-8760.27 this takes the form

$$\left(\frac{\phi}{\phi_0}\right)^2 = 1.065 - 0.0486\exp\left(-\frac{4.22\times10^2}{T}\right)t - 1.487\times10^{-6}\exp\left(-\frac{0.639}{T^2}\right)t^2 \quad (30)$$

and for LL-8461.27

$$\left(\frac{\phi}{\phi_0}\right)^2 = 0.968 - 2.844\exp\left(-\frac{1.269\times10^3}{T}\right)t - 0.563\times10^{-6}\exp\left(-\frac{0.932}{T^2}\right)t^2 \quad (31)$$

3. Extensive experimental trials have shown that once formed, the bubbles exhibit practically no movement to the free surface. This is explained in terms of the high viscosity of the polymer relative to the buoyancy forces.

References

1. R. J. CRAWFORD, *Progr. Rubb. Plast. Technol.* **6** (1990) 1.
2. J. A. SCOTT, PhD thesis, Queen's University of Belfast (1986).
3. L. A. McKENNA, in "Technical Papers, Regional Technical Conference", Society of Plastics Engineers, October, 1965 p. 33.
4. "Rotational moulding of microthene polyethylene powders" (USI Chemicals Co., 1965).
5. R. E. GULLICK, G. F. KIRKPATRICK and R. J. PECHA, *Modern Plastics* (May 1962) p. 102.
6. R. J. CRAWFORD and J. A. SCOTT, *Plast. Rubb. Process. Appl.* **7** (2) (1987) 85.
7. C. D. SPENCER, *Soc. Plast. Eng. J.* **18** (1962) 774.
8. R. E. DUNCAN, in Proceedings of Symposium II on Rotational Moulding with Linear Powdered Polyethylene, US Industrial Chemical Co., June 1966.
9. R. L. REE, in Proceedings, Society of Plastics Engineers, 27th Annual Technical Conference, May 1969, p. 567.
10. L. XU, "Theoretical and Experimental Study of Physical and Thermal Characteristics of Plastic Powders used for Rotomoulding", 1st year report (Queen's University of Belfast, 1991).
11. "Now clear PC rotomoulded parts", *Modern Plast. Int.* (November 1980) 30.
12. J. J. BREZINSKI, K. D. CAVENDER and G. V. OLHOFT, *Plast. Technol.* (October 1973) 75.
13. L. XU, "The Studies of Thick Wall Moulding", Department of Mechanical Engineering report No. 1 (Queen's University of Belfast, 1991).
14. J. M. McDONAGH, in Proceedings of Regional Conference, Society of Plastics Engineers March 1969, p. 35.
15. S. R. PAQUETT, *ibid.* p. 13.
16. V. WRIGHT, *Modern Plast.* (May 1969) p. 75.
17. F. J. RATTI, "How to buy rotational moulding machinery", Plastics Technology Processing Handbook (October 1969) p. 201.
18. G. E. CARROW, *Appl. & Process* (February 1974).
19. *Idem, Plast. Des. Process.* (March 1974).
20. M. A. RAO and J. L. THRONE, *Polym. Eng. Sci.* **12** (1972) 237.
21. D. RAMAZZOTTI, in Proceedings of Regional Technical Conference, Society of Plastics Engineers, October 1975, p. 43.
22. J. L. MACADAMS, *Plast. Technol.* **22** (June 1976) 45.
23. H. R. HOWARD, in Proceedings of Conference, Association of Rotational Moulders, Chicago, October 1977.
24. M. A. RAO and J. L. THRONE, in Proceedings of Conference, Society of Plastics Engineers, May 1972, p. 759.
25. R. C. PROGELHOF, G. CELLIER and J. L. THRONE, in Proceedings of Annual National Technical Engineering Conference, Society of Plastics Engineers, 1982, p. 762.
26. P. Y. KELLY, "A Microscopic Examination of Rotational Polyethylene" (DuPont, Canada, undated).
27. J. FRENKEL, *J. Phys. (USSR)* **9** (1945) p. 385.
28. G. C. KUCZYNSKI and J. ZAPLATYNSKYJ, *J. Amer. Ceram. Soc.* **39** (1956) 349.
29. G. C. KUCZYNSKI, B. NEUVILIE and H. P. TONER, *J. Appl. Polym. Sci.* **14** (1970) 2069.
30. J. F. LONTZ, in "Fundamental Phenomena in the Material Sciences", Vol. 1, edited by L. J. Bonis and H. H. Hansner, (Plenum, New York, 1964) Ch. 1.
31. M. NARKIS, *Polym. Eng. Sci.* **19** (1979) 889.
32. N. ROSENZWEIG and M. NARKIS, *ibid.* **21** (1981) 582.
33. *Idem, ibid.* **21** (1981) 1167.
34. *Idem, ibid.* **23** (1983) 32.
35. J. F. LONTZ, in Proceedings of 4th Delaware Valley Regional Meeting, American Chemical Society, Philadelphia, Pennsylvania, January 1962.
36. C. H. GREENE and R. F. GAFFNEY, *J. Amer. Ceram. Soc.* **46** (1959) 271.
37. R. H. DOREMUS, *ibid.* **43** (1960) 655.
38. H. S. CARSLAW and J. C. JAEGER, "Conduction of Heat in Solids" (Clarendon Press, Oxford, 1947).
39. C. ZENER, *J. Appl. Phys.* **20** (1949) 950.
40. F. C. FRANK, *Proc. Roy. Soc. (London) A* **201** (1950) 586.
41. A. S. MICHAELS and H. J. BIXLER, *J. Polym. Sci., Letters* (1961) 413.
42. J. J. McKEOWN, "INTERSECT: An Outline User Guide", Internal report (Department of Engineering Mathematics, Queen's University of Belfast, 1991).

Received 17 September 1991
and accepted 16 June 1992